

The Fractal Dimension of Scalar Surfaces in Turbulent Jets

K.R. Sreenivasan and R.R. Prasad

Mason Laboratory, Yale University, New Haven, CT 06520

1. Introduction

If we regard any single realization of an unbounded turbulent flow as an object of scientific interest, it is natural to inquire about ways of describing its geometric features. We are especially interested in the geometry of various surfaces such as the vorticity interface (that is, the conceptual surface separating domains of intense and zero vorticity fluctuations), iso-concentration surfaces (in non-reacting as well as reacting flows), iso-velocity surfaces, and iso-dissipation surfaces. A common property of such surfaces is that they are highly convoluted on many scales, and possess complex shapes. This complexity defeats attempts to describe them by means of classical geometry, and one naturally wonders whether the fractal geometry developed by Mandelbrot (in many papers and his 1982 book) is appropriate for the purpose. Mandelbrot had earlier speculated that the self-similarity expected to hold in turbulence (according to the conventional wisdom succinctly described by Richardson's (1922) rhyme) permits surfaces of the type mentioned earlier to be described by fractals. In this paper we substantiate this speculation, using the particular case of scalar interfaces in turbulent jets as an example. We also show that the experimentally obtained fractal dimension is consistent with deductions from the principle of Reynolds number similarity (that is, negligible dependence on viscosity of global properties such as the overall growth rates of turbulent flows). This paper should be considered a condensed version of our earlier publications (Sreenivasan & Meneveau 1986, Sreenivasan et al. 1987a,b – referred to respectively as I, II and III below); moreover, we restrict ourselves only to turbulent jets here. Within these constraints, however, some aspects are discussed here in somewhat better detail than in the references cited above.

To sharpen our question somewhat, we show in figure 1 a thin longitudinal slice along the axis of a turbulent jet of water emerging from a well-contoured nozzle of circular cross-section into a tank of still water. The jet was made visible by mixing a small amount (of the order of 10 parts per million) of a fluorescing dye (sodium fluorescein) into the nozzle fluid, and exciting fluorescence by illuminating



Figure 2. The boundary of the jet crosssection given in figure 1, determined by prescribing a threshold on brightness (\sim the concentration of the nozzle fluid). Also shown is a typical line intersection of the boundary; this will be discussed later in the text

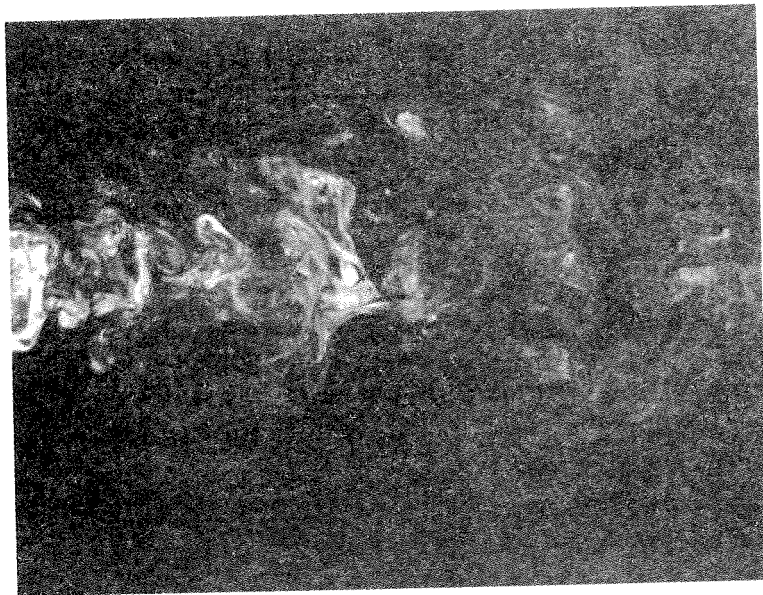


Figure 1. A thin axial section of the nozzle fluid marked by a fluorescing dye. The jet Reynolds number (based on the nozzle diameter and velocity) is about 4000. The picture covers between 8 and 24 diameters from the nozzle

a thin section of the flow by a sheet of light. Care was taken to ensure that the fluorescence was not saturated. The light source was a pulsed Nd:YAG laser which has a pulse width of the order of 8 ns (which is small enough to freeze the motion), and power density of up to $2 \times 10^7 \text{ J} \cdot \text{s}^{-1}$ per pulse; the light sheet had a thickness of the order of 200-250 μm , which is on the order of the estimated Kolmogorov scale (that is, the smallest dynamical scale in the flow). For this reason, it is legitimate to consider the plane intersection 'mathematically thin'. The visualized region extends from 8 to 24 nozzle diameters, and was captured on a solid state CCD camera with a pixel array of 1300 (vertical) \times 1000 (horizontal), yielding a resolution of 150 μm^2 .

The picture shows a number of geometrically interesting features, one of which relates to the boundary that separates the nozzle fluid from the ambient tank fluid. (Some other aspects are described in I and Meneveau & Sreenivasan 1987.) The boundary is convoluted on a variety of scales, and appears to be disconnected at many places. We recognise the possibility that some out-of-plane connections may exist and that the boundary is indeed connected; clearly, to establish this aspect properly, at least several simultaneous sections would be needed and, in their absence, we shall refrain from further comments on it. In any case, one can imagine in three dimensional space a surface that separates the nozzle fluid from the ambient tank fluid, a surface whose section by a plane is seen in figure 1. This surface is of interest to us for many reasons, the primary one being that its geometry (which itself is a consequence of some dynamical constraints) will influence the amount of mixing that occurs between the nozzle and tank fluids. For example, if the tank fluid were slightly acidic and the jet fluid slightly alkaline, the surface geometry will govern the amount of product formed as a result of reaction between the acid and the base. (The validity of this argument should be obvious for diffusion limited mixing and, as shown in II, is also applicable while considering convective effects.)

As mentioned earlier, our objective is to characterize this surface (and in general all surfaces of interest in turbulent flows) by fractals; a primary property of a fractal surface being its fractal dimension, we want to measure it. We shall obtain the fractal dimension of the boundary seen in figure 1, and later examine the sense in which it relates to the fractal dimension of the surface embedded in three dimensions.

2. Experiments and Results

a. Method of measurement of fractal dimension

The first step is to specify how the boundary can be defined for further processing. Complex algorithms can be developed for the purpose, but we shall

show that it is adequate to use simple criteria based on the brightness threshold in the picture (which, in a digitized image, is directly proportional to the concentration threshold on the nozzle fluid).

Figure 2 shows the computer-drawn boundary obtained by setting the threshold at a brightness level that seems more or less satisfactory. One can now apply one of several techniques (described, for example, in Mandelbrot's book) to determine the fractal dimension of the boundary so marked. We have used both the box-counting and co-dimension methods. The co-dimension method was described in detail in I. In the box-counting methods, also briefly described in I, we cover the whole plane of figure 2 with area elements of varying sizes, count only the fraction of elements N containing the boundary, and plot $\log N(r)$ as a function of logarithm of the 'box' size r ; if the boundary is a fractal, we should expect an extensive straight part in this log-log plot, whose negative slope is the fractal dimension. A typical result (figure 3a) shows that this is indeed the case, the straight part extending from the smallest scale resolved here to approximately a scale of the order of the nozzle diameter, giving a fractal dimension of 1.35 for the boundary. (It is worth remarking that the programs for computing fractal dimensions have been checked extensively on several mathematically generated fractal sets of known dimension.)

We appreciate that some minor ambiguities exist in defining the interface merely by means of a threshold, and so measurements have been repeated for a number of thresholds on several realizations of the jet. Figure 3b shows a plot of some of these results. It is clear that there exists a wide range of threshold values over which the fractal dimension of the boundary is essentially independent of the threshold, and that the mean value is 1.35. The spread of the data around this mean value is roughly in the range ± 0.05 . Figure 3c shows that the range of scale similarity (that is, the range of scales over which the log-log plot has a straight part) varies somewhat with the threshold, but is generally about 1.5 to 2 decades.

We have shown in II that similar experiments in other prototypical turbulent flows yield the same results. This will not be repeated here. We shall also not repeat another result from III showing that flow slices taken in different orientations possess approximately the same fractal dimension.

b. Fractal dimension from intersections

We may now ask how the fractal dimension from planar intersections is related to the fractal dimension D of the surface itself – this being our major concern. This general problem has been discussed in the literature, and specific results are available for special cases (see Marstrand 1954, whose results have been

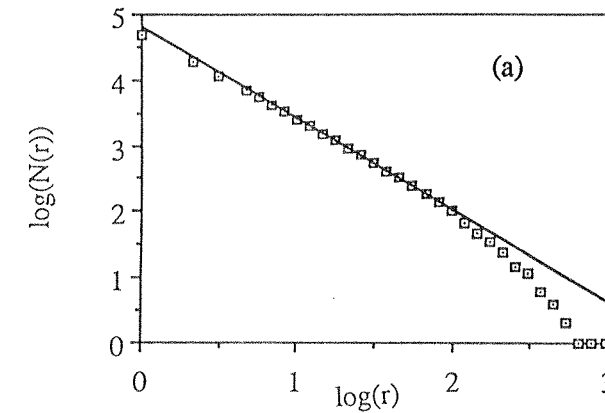


Figure 3a. The log-log plot of the area elements ("boxes") of size r containing the interface. The negative slope of the straight part gives the fractal dimension of the boundary ($=1.35$)

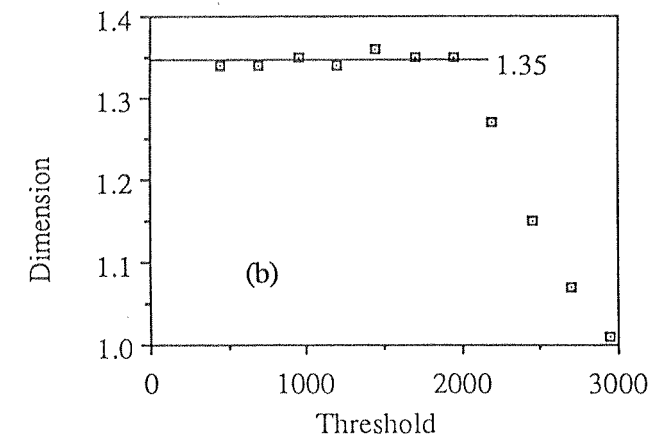


Figure 3b. Fractal dimension of the interface as a function of threshold chosen to generate the interface. The abscissa is in units of the dynamic range of the camera (0-4096)

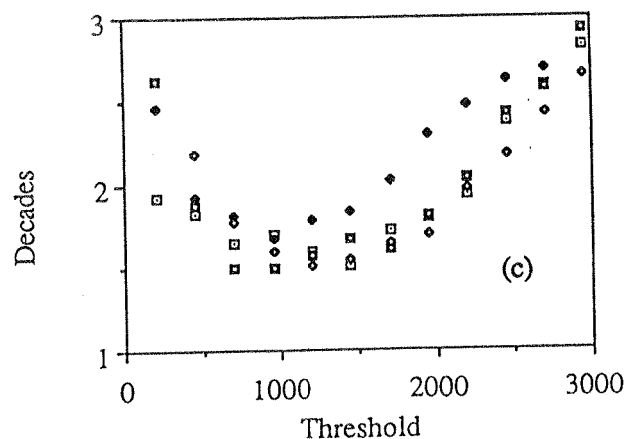


Figure 3c. Scaling range in decades for each threshold for a number of realizations. For the Reynolds numbers typical of most experiments in present series (about 5000 based on the nozzle diameter and velocity), the typical outer/inner scale ratio is about 100

generalized by Mattila 1975). The equivalent result in the present context, as stated by Mandelbrot (1982, p. 366), relates to the additive properties of codimensions in the intersection problems. Specifically, if S_1 and S_2 are two *independent* sets embedded in a space of dimension d , and if $\text{codimension}(S_1) + \text{codimension}(S_2) < d$, the codimension of the intersection of S_1 and S_2 is equal to the sum of the codimensions of S_1 and S_2 . For a fractal set F embedded in three dimensional space and intersected by a plane, the above statement implies that the dimension of the intersected set is one less than the dimension of F .

We have shown that the fractal dimension of the boundary in longitudinal (that is, streamwise) sections of the jet is 1.35, and remarked that boundaries created by orthogonal sections possess approximately the same fractal dimension. It then follows that the fractal dimension of the surface is one greater than 1.35, or $D = 2.35$.

It may be useful to expand briefly on the result that the fractal dimension of intersections is independent of the orientation of the intersecting plane. Intuitively, this result can be expected to be valid if the intersected object is fractally isotropic. In general, flows considered here do have a preferential direction, and it is logical to think that the interfaces are that way also. We should, however, emphasize two points: First, the possible anisotropic properties of the interface will be confined essentially to the largest scales in the flow, these being on the order of the jet width (and larger). Secondly, the smaller scales for which fractal-like behavior has been found are expected to be more or less isotropic, thus explaining our observation. Although we have been unable to take simultaneous orthogonal sections, measurements with independent sections have shown that the anisotropy may affect the precise range of scale similarity in two orthogonal planes but not the fractal dimension itself.

c. Off-axis jet sections

Figures 4 and 5 are two independent jet sections obtained one and two diameters off-axis. A cursory examination of these figures in conjunction with figure 1 suggests that our knowledge of the turbulent structure will remain incomplete unless a scheme can be devised for three dimensional imaging of the flow. Our limited purpose here is to point out that the fractal dimension of the boundary in these pictures is also about 1.35, and is independent of the threshold (perhaps even more accurately than for the axial sections).

d. Line intersections

The principle of additive codimensions in the context of line intersections

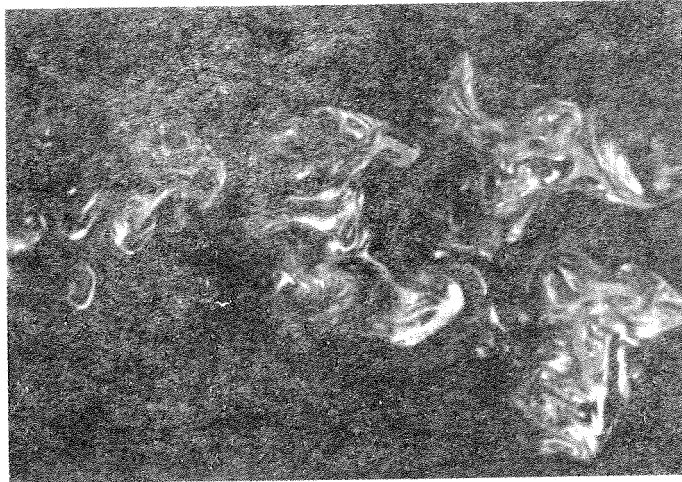


Figure 5. A thin section of the nozzle fluid marked by the fluorescing dye, two diameters off axis

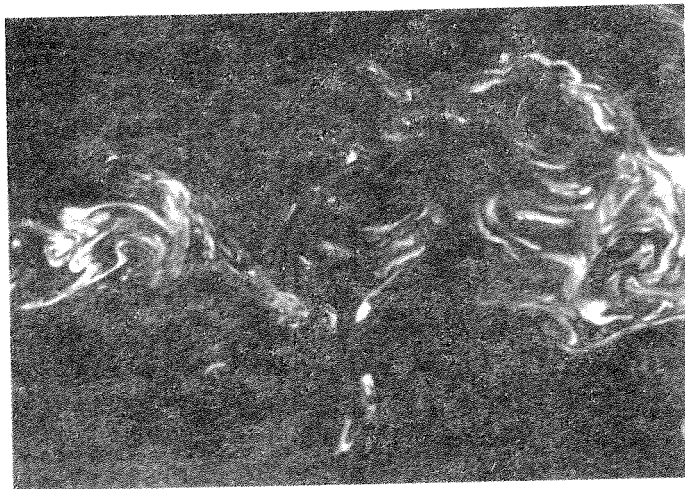


Figure 4. A thin section of the nozzle fluid marked by the fluorescing dye, one diameter off-axis

implies that the fractal dimension of line intersections is two less than that of the surface. By using box counting methods as before, one can compute the fractal dimension of the set of discrete points corresponding to the intersection of the interface by a given line (see figure 2 for examples). Figure 6 shows the measured fractal dimension of line intersections (passing through a fixed point) as a function of the orientation of the intersecting line. The mean value is about 0.37 (giving $D = 2.37$). The figure also shows that line cuts passing through other points also yield the same result.

e. Summary

We should emphasise that, within the uncertainty of measurement, we do not attach too much significance to the differences of the fractal dimension estimated from one and two dimensional cuts. It then follows that the fractal dimension of scalar interfaces in fully developed regions of the turbulent jet is 2.35 ± 0.05 . Results given in I and III show that this conclusion is valid for other prototypical flows also. The result is thus a general one, and demands an interpretation based on broad considerations. This is attempted in section 3. However, before we do that, we digress briefly on an independent aspect concerning the fractal dimension in the developing regions of the jet.

f. Fractal dimension in the developing regions

At least at low Reynolds numbers, the jet is circular in crosssectional shape as it emerges from the nozzle, and the geometry of the surface is a simple conical section; common experience tells us that the interface dimension will be 2. Far enough downstream of the nozzle, however, the jet becomes turbulent and, as we have shown, the interface there attains a fractal dimension of about 2.36. It is of some interest to ascertain the variation of the fractal dimension with axial distance. Without remarking on the significance of the result, we merely present the experimental results in figure 7. Similar results for the countercurrent mixing layer can be found in II.

3. Mixing and Reynolds number similarity

a. Diffusive transport

Let us consider transport by diffusion across interfaces of the type discussed so far. Here, we shall completely ignore convective aspects due to the relative motion of the interface, the chief justification being that their inclusion has been shown in II to have no effect on the conclusions. The following argument holds equally well for

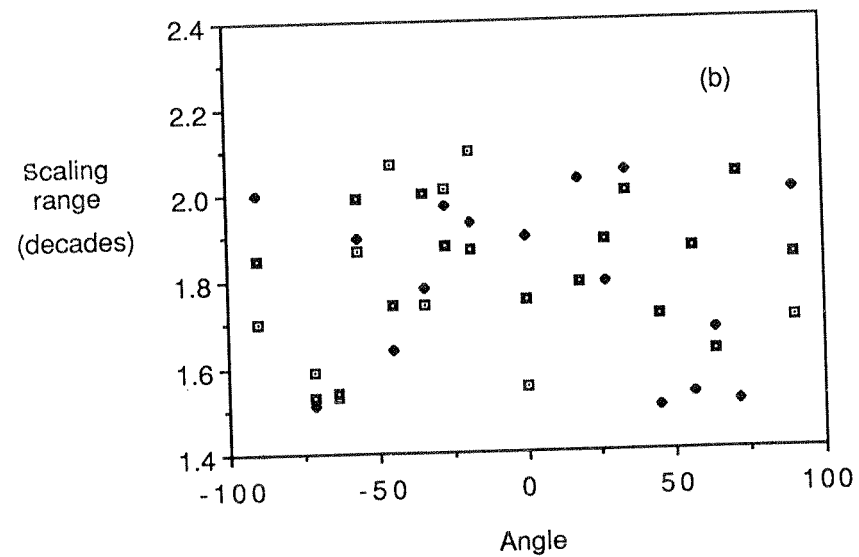
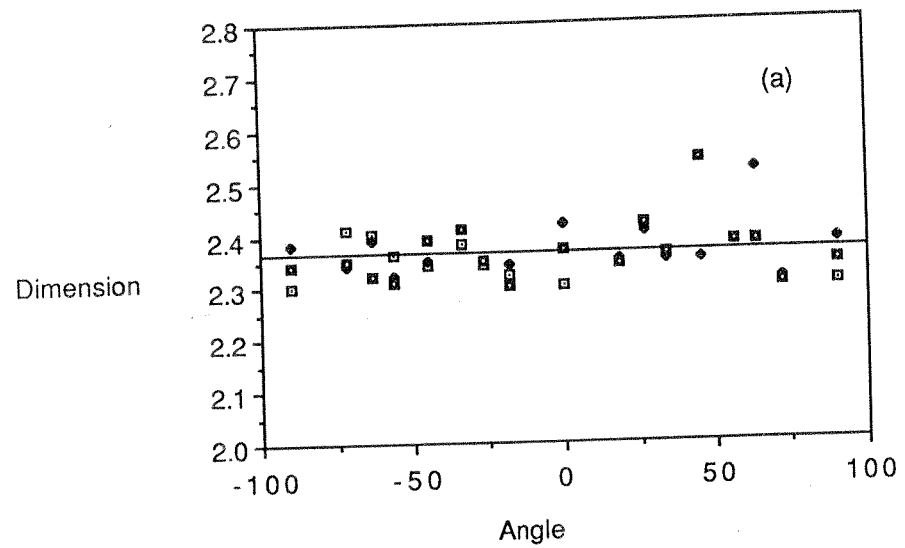


Figure 6. (a) Typical results from one-dimensional cuts passing through a fixed point as a function of the orientation of the intersecting line; different symbols correspond to line cuts passing through different points. Figure 6(b) indicates the observed scaling range

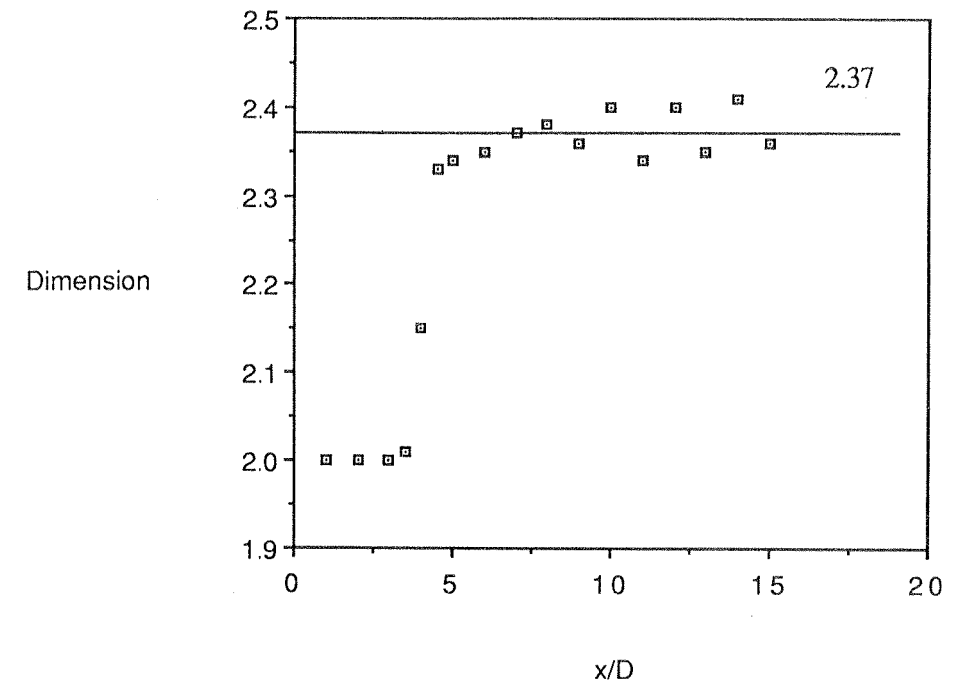


Figure 7. The fractal dimension as a function of the axial distance in the developing region of the jet. The Reynolds number is about 2000. The nearly discontinuous jump occurring at about 4.5 diameters coincides with the visibly sudden change in the smoothness of the scalar surface

jets as well as other flows.

The diffusive flux is given by the product of the surface area, the concentration gradient normal to the surface and the molecular diffusivity. For fractals, the surface area S increases with the resolution of measurement r according to the relation (Mandelbrot 1982)

$$S \sim r^{2-D}. \quad (1)$$

In all practical circumstances, the scale range over which (1) holds is bounded by cut-offs on both ends. For surfaces in turbulent flows, the outer cut-off is expected to occur at scales comparable to the integral scale, L , of turbulence, while the inner cut-off occurs at the smallest dynamical scale. For the vorticity interface, the appropriate inner scale is the Kolmogorov scale $\eta = (\nu^3/\langle \epsilon \rangle)^{1/4}$, where $\langle \epsilon \rangle$ is the average rate of the turbulent energy dissipation. This was shown to be the case in II. For scalars with Schmidt number ($= \nu/D$, where ν is the kinematic viscosity of the fluid and D is the mass diffusivity of the scalar) greater than unity, the relevant inner cut-off occurs at the Batchelor scale, $\eta_b = \eta Sc^{-1/2}$. The existence of a finite inner cut-off means that, as the surface area gets measured by covering it with increasingly finer area elements, a point is reached at which convolutions of even finer scales no longer exist, so that, thereafter, the area does not increase with increasing fineness of resolution; instead, it will saturate (abruptly in an ideal situation) at the maximum value corresponding essentially to the inner cut-off. The true surface area S_T of a fractal surface with finite inner cut-off is thus given (to within a constant) by the knowledge of the fractal dimension, and the inner cut-off r_i which theoretically truncates the power-law behaviour. Thus,

$$S_T = S_0 (r_i/L)^{2-D} \quad (2)$$

where S_0 is some normalizing area. If the area levels off at L and beyond, S_0 becomes the surface area measured with the resolution equal to L .

It was shown in II that the characteristic velocity and concentration gradient across interfaces are of the order u'/η and c'/η_b respectively, u' and c' being the root-mean-square velocity and concentration fluctuations. Combining this with (2), an expression for the flux of momentum across the interface can be written as

$$\nu S_T (u'/\eta). \quad (3)$$

Defining the characteristic Reynolds number $Re = u'L/\nu$, we may note that $\eta/L \sim$

$Re^{-3/4}$, and use equation (2) for the interface area S_T to write (after a little algebra) that the

$$\text{diffusive flux of momentum} \sim S_0 U_c^2 (u'/U_c)^2 Re^{3(D-7/3)/4}. \quad (4)$$

Note that S_0 , U_c and (u'/U_c) are all independent of Reynolds number; U_c is a characteristic velocity, for example the centerline defect velocity for wakes, the centerline excess velocity for jets, the velocity difference between the two streams for mixing layers, and the friction velocity (equal in kinematic units to the square root of the wall shear stress) for boundary layers. For non-unity Schmidt numbers, the corresponding result for the flux of a species with concentration difference ΔC is given by

$$\text{diffusive flux of contaminant} \sim S_0 (U_c \Delta C) (u'c'/U_c \Delta C) Re^{3(D-7/3)/4} Sc^{0.5(D-3)}, \quad (5)$$

where $c'/\Delta C$ is another constant. It was shown in II that the only effect of incorporating convective effects is to alter the constants of proportionality in (4) and (5).

b. The fractal dimension

Now, it is well known that all fluxes (mass, momentum, energy) must be independent of Reynolds number in fully turbulent flows – the so-called Reynolds number similarity. This is merely a statement of the observed fact that the growth rates of turbulent flows of a given configuration are independent of fluid viscosity. According to (4) and (5) the Reynolds number similarity requires that

$$D = 7/3 \quad (6)$$

for both the vorticity and scalar interfaces, in rough agreement with experiments. (For preliminary experiments on vorticity interfaces, see I.)

In the above arguments we have assumed that it is appropriate to use a common characteristic velocity or concentration gradient everywhere along the interface. This is strictly not true, at least because the interface thickness varies from place to place due to the intermittent nature of the dissipation rate ϵ . Furthermore, it is implied that the globally averaged dissipation rate is the same as that averaged in the neighbourhood of the interface alone (roughly the 'superlayer' of Corrsin & Kistler, 1955). These two issues were addressed in detail in II, where it was shown that the intermittent nature of the dissipation near the interface is statistically the

same as that elsewhere, and that the inclusion of the intermittency will alter the interface dimension from $7/3$ to about 2.36. This latter estimate is in excellent agreement with our experimentally determined mean value. It is worth mentioning that the reason for the relatively small correction is that the interface thickness depends on the quarter power of the dissipation, and so the strong variabilities in ϵ do not translate to comparable variations in the interface thickness.

Acknowledgements

Discussions with C. Meneveau and R. Ramshankar have been very beneficial. We are thankful for financial support to the Air Force Office of Scientific Research and the Defence Advanced Research Projects Agency.

References

- Corrsin, S. & Kistler, A.L. (1955) Free-stream boundaries of turbulent flows, NACA Tech. Report 1244.
- Mandelbrot, B.B. (1982) *The Fractal Geometry of Nature*. (Freeman; San Francisco)
- Marstrand, J.M. (1954) Some fundamental geometrical properties of plane sets of fractal dimensions, *Lond. Math. Soc.* **3**, 257.
- Mattila, P. (1975) Hausdorff dimension, orthogonal projections and intersections with planes, *Ann. Acad. Sci. Fenn. Ser. A I Math.* **1**, 227.
- Meneveau, C.M. & Sreenivasan, K.R. (1987) The multifractal dissipation field in turbulent flows, In *Physics of Chaos and Systems Far from Equilibrium*, (eds. Minh-Doung Van & B. Nichols (North-Holland, Amsterdam).
- Richardson, L.F. (1922) *Weather Prediction by Numerical Process*. (Cambridge University Press)
- Sreenivasan, K.R. & Meneveau, C. (1986) The fractal facets of turbulence *J. Fluid Mech.* **173**, 357.
- Sreenivasan, K.R., Ramshankar, R. & Meneveau, C. (1987) Mixing, entrainment, and fractal dimension of interfaces in turbulent flows, Submitted for publication.
- Sreenivasan, K.R., Prasad, R.R., Meneveau, C. & Ramshankar, R. (1987) The geometry of scalar interfaces in fully turbulent flows, To appear in *Fractals in Geophys.* (Special issue of *J. Pure and Applied Geophys.* eds. C. Scholz & B.B. Mandelbrot, Birkhauser.)

Four more survey lectures were presented during the Symposium:

H. Hornung "Sources of Vorticity",

S.J. Putterman "Universal Power Spectra for Turbulence and Applications",

A.K. Rebrov "Transational Relation and Problems of Gasdynamics Separation",

A.M. Yaglom, B.A. Kader "Statistical Description of Turbulence in Nonstratified and Unstably Stratified Boundary Layer".

These papers, however, were not submitted for publication in this volume.

PAŃSTWOWE WYDAWNICTWO NAUKOWE
WARSZAWA 1989 R.

Wydanie I. Nakład 310 + 90 egz. Ark. wyd. 11,75. Ark. druk. 13,75.
Papier offsetowy kl. III, 80 g, 70 × 100 cm. Materiały przygotowane
przez Zleceniodawcę oddano do reprodukcji w czerwcu 1989 r.

Druk ukończono w czerwcu 1989 r. Zam. 418/89, A-94.

ZAKŁAD GRAFICZNY WYDAWNICTW NAUKOWYCH
Łódź, ul. Żwirki 2